



PEARL

The distribution of deep-sea sponge aggregations in the North Atlantic and implications for their effective spatial management.

Howell, Kerry Louise; Piechaud, Nils; Downie, Anna Leena; Kenny, Andrew

Published in:

Deep Sea Research Part I: Oceanographic Research Papers

DOI:

[10.1016/j.dsr.2016.07.005](https://doi.org/10.1016/j.dsr.2016.07.005)

Publication date:

2016

Link:

[Link to publication in PEARL](#)

Citation for published version (APA):

Howell, K. L., Piechaud, N., Downie, A. L., & Kenny, A. (2016). The distribution of deep-sea sponge aggregations in the North Atlantic and implications for their effective spatial management. *Deep Sea Research Part I: Oceanographic Research Papers*, 0(0). <https://doi.org/10.1016/j.dsr.2016.07.005>

All content in PEARL is protected by copyright law. Author manuscripts are made available in accordance with publisher policies. Wherever possible please cite the published version using the details provided on the item record or document. In the absence of an open licence (e.g. Creative Commons), permissions for further reuse of content should be sought from the publisher or author.

1 Title: The distribution of deep-sea sponge aggregations in the North Atlantic and implications
2 for their effective spatial management.

3 * Kerry-Louise Howell¹, Nils Piechaud¹, Anna-Leena Downie², Andrew Kenny²

4

5 ¹Marine Biology & Ecology Research Centre, Marine Institute, Plymouth University,
6 Plymouth, PL4 8AA, UK.

7 ²Centre for the Environment, Fisheries and Aquaculture Science (Cefas), Pakefield Road,
8 Lowestoft NR33 0HT, UK

9 Correspondence author's name:

10 Kerry Howell, email: Kerry.Howell@plymouth.ac.uk

11

12

13 Key words: Deep-sea; habitat suitability mapping; species distribution modelling; sponges;
14 marine conservation; environmental management;

15

16

17 Abstract:

18 Sponge aggregations have been recognised as key component of shallow benthic
19 ecosystems providing several important functional roles including habitat building and
20 nutrient recycling. Within the deep-sea ecosystem, sponge aggregations may be extensive
21 and available evidence suggests they may also play important functional roles, however data
22 on their ecology, extent and distribution in the North Atlantic is lacking, hampering
23 conservation efforts. In this study, we used Maximum Entropy Modelling and presence data
24 for two deep-sea sponge aggregation types, *Pheronema carpenleri* aggregations and ostur
25 aggregations dominated by geodid sponges, to address the following questions: 1) What
26 environmental factors drive the broad-scale distribution of these selected sponge grounds? 2)
27 What is the predicted distribution of these grounds in the northern North Atlantic, Norwegian
28 and Barents Sea? 3) How are these sponge grounds distributed between Exclusive
29 Economic Zones (EEZs) and High Seas areas? 4) What percentage of these grounds in
30 High Seas areas are protected by the current High Seas MPA network? Our results suggest
31 that silicate concentration, temperature, depth and amount of particulate organic carbon are
32 the most important drivers of sponge distribution. Most of the sponge grounds are located
33 within national EEZs rather than in the High Seas. Coordinated conservation planning
34 between nations with significant areas of sponge grounds such as Iceland, Greenland and
35 Faroes (Denmark), Norway (coastal Norway and Svalbard), Portugal and the UK, should be
36 implemented in order to effectively manage these communities in view of the increasing level
37 of human activity within the deep-sea environment.

38 1. Introduction

39 Sponges are a key component of marine benthic ecosystems from shallow tropical coral
40 reefs to deep-sea systems, providing a number of important functional roles. Studies in
41 shallow waters have suggested sponge communities create complex habitats supporting
42 high biodiversity, provide refuge for fish, are a source of novel chemical compounds, and
43 have an important role in biogeochemical cycling (Bell 2008; Maldonado et al., 2016). Deep-
44 sea sponge aggregations, although less studied than their shallow water counterparts, show
45 evidence of having similar important functional roles.

46 Within the North Atlantic there are three widely accepted and clearly defined deep sea
47 sponge habitat types, *Pheronema carpenleri* (Thomson 1869) aggregations (Rice et al.,
48 1990), boreal ostur, and cold water ostur (Klitgaard and Tendal 2004). While there is no
49 doubt other sponge aggregations do exist, these have not yet been defined in the peer
50 reviewed literature. *P. carpenleri* is a hexactinellid (glass sponge) that can form aggregations
51 on fine sediments with densities of up to 1.53 individuals/m² as seen on the Goban Spur
52 (Hughes and Gage 2004). These aggregations are associated with an increase in
53 abundance and richness of macrofauna within spicule mats and sponge bodies providing
54 habitat complexity and a hard substrate for epifauna colonization , (Rice et al., 1990; Bett
55 and Rice 1992). They are thought to be associated with areas of high productivity, and
56 possibly proximate to regions of enhanced bottom tidal currents which aid in resuspension of
57 organic matter (Rice et al., 1990; Whiteet al., 2003).

58 Another widely recognised deep-sea sponge aggregation is ‘ostur’ or ‘cheese bottom” as
59 defined by (Klitgaard and Tendal 2004). These authors recognise two main types of ostur: a
60 boreal ostur, which occurs around the Faroe Islands, Norway, Sweden, parts of the western
61 Barents Sea and south of Iceland; and a cold water ostur, which is found north of Iceland, in
62 most of the Denmark Strait, off East Greenland and north of Spitzbergen. Both ostur types
63 are characterised by sponges of the genus *Geodia* Lamarck, 1815. Boreal ostur consist of

64 *Geodia barretti* Bowerbank 1858, *Geodia macandrewii* Bowerbank 1858, *G. atlantica*
65 (Stephens, 1915) and *G. phlegraei* (Sollas 1880), whilst cold water ostur is formed by *G.*
66 *hentscheli* Cárdenas, Rapp, Schander and Tendal 2010 (referred to as *G. mesotriaena*) and
67 *G. parva* (Hansen 1885) (referred to as *Isops phlegraei pyriformis* but identified as *G. parva*
68 in Cárdenas et al., (2013)) . Maps of the distribution of ostur, determined largely from
69 fisheries trawl samples, were compiled by (Klitgaard and Tendal 2004), while more recently
70 Cárdenas et al, (2013) have summarised known locations of characterising geodid species
71 on maps.

72 Deep sea sponge habitats are also thought to play a key role in nutrient recycling as a result
73 of the large quantities of water they filter (Reiswig, 1971; Reiswig, 1974). Sponges are
74 suspension feeders and recent studies have demonstrated the importance of sponge
75 feeding to benthic-pelagic coupling in the deep sea (Pile and Young 2006; Yehel et al., 2007),
76 with sponges representing an important link between carbon in the water column in the form
77 of ultraplankton and picoplankton (Reiswig 1975), dissolved organic carbon (Yahel et al.,
78 2003) and viral particles (Hadas et al., 2006), and the benthos. Sponges may enable carbon
79 flow to higher trophic levels through predation (Wulff 2006) and respiration rates are 9 times
80 higher on sponge grounds than surrounding sediments (Cathalot et al., 2015). In addition,
81 areas of high sponge abundance may play a key role in global Silicate cycling (Maldonado et
82 al., 2005) the importance of which might be geographically variable (Bell 2008). Further,
83 Hoffmann et al., (2009) postulated that all sponge aggregations may function as so far
84 unrecognized sinks for inorganic nitrogen.

85 The range of ecological functions provided by deep-sea sponge aggregations has resulted in
86 these habitats being considered of conservation importance under United Nations General
87 Assembly Resolution 61/105” and under Annex V of the Oslo-Paris (OSPAR) Convention for
88 the Protection of the Marine Environment of the North East Atlantic. Thus stakeholders are
89 required, in respect of areas where vulnerable marine ecosystems (VMEs) are known to
90 occur or are likely to occur based on the best available scientific information, to close such

91 areas to bottom fishing and ensure that such activities do not proceed unless conservation
92 and management measures have been established to prevent significant adverse impacts
93 on VMEs (UNGA 61/105).

94 Despite these policy provisions, progress in the protection of deep-sea sponge aggregations
95 is slow. Several nations and the Northwest Atlantic Fisheries Organization (NAFO) have
96 recently recommended or implemented area closures for the protection of sponge habitats in
97 response to UNGA Resolution 61/105. To date however, no OSPAR marine protected areas
98 (MPAs) have been designated specifically for the protection of these habitats. Part of the
99 reason for the slow progress is likely to be the more limited spatial location data for deep sea
100 sponge habitats (Rodríguez et al., 2007), although indicative maps of the distribution of
101 some types of sponge grounds have existed for some time (Klitgaard and Tendal 2004).

102 While the production of point based distribution maps are a critical first step in developing
103 environmental management strategies, predictive habitat modelling provides a means to
104 produce full coverage spatial data where distribution information is lacking (Elith and
105 Leathwick 2009; Galparsoro et al., 2009; Dambach and Rodder 2011; , , Robinson et al.,
106 2011). The resulting predictions may then be used to support conservation management
107 decisions (Kenchington and Hutchings 2012) .

108 Predictive modelling of the distribution of a biological 'habitat' such as a deep-sea sponge
109 aggregation may be achieved in a variety of ways. Where the habitat is formed by a single
110 dominant species, two different approaches have been used. The first models the
111 distribution of the species (Davies et al.,2008, Dolan et al., 2008, Guinan et al., 2009), the
112 second models the distribution of the habitat (Ross and Howell, 2013; Ross et al., 2015).

113 Where both approaches have been used results suggest that predicted habitat distribution is
114 a highly restricted subset of predicted species distribution (Howell et al., 2011, Rengstorf et
115 al., 2013). Where a 'habitat' is composed of a distinct assemblage of species, the distribution
116 of that assemblage may be modelled (Degraer et al., 2008, Gonzalez-Mirelis and Lindegarth

117 2012, Piechaud et al., 2015), alternatively the distribution of key indicator species may be
118 modelled and the resulting maps overlaid highlighting areas of overlap as potential habitat
119 distribution (Ferrier and Guisan 2006; Rinne et al., 2014)

120 This study uses Maximum Entropy Modelling, considering both species and habitat based
121 approaches, to address the following questions:

- 122 1) What environmental factors drive the broad-scale distribution of ostur and
123 *Pheronema carpenleri* sponge grounds?
- 124 2) What is the predicted distribution of these grounds in the northern North Atlantic,
125 Norwegian and Barents Sea?
- 126 3) How are these sponge grounds distributed between EEZ and High Seas areas?
- 127 4) What percentage of these grounds in High Seas areas are protected by the current
128 High Seas MPA network?

129

130 2. Methods

131 2.1. Study Area

132 The study is focused on the North Atlantic deep sea areas (200 to 5000 meters deep) off the
133 Canadian coast, the Azores and the Iberian Peninsula to Baffin Bay, Greenland and Iceland,
134 the Greenland Sea and western part of Barents Sea off the coasts of Spitzberg (Fig. 1). This
135 region was chosen to encompass an area where sufficient data are available on presence
136 and absence of ostur, geodids, and *P. carpenleri*. Although geodid sponges are very
137 common in fjords (Klitgaard and Tendal 2004), coastal regions were not included as a result
138 of both the resolution and coverage of some of the environmental layers.

139

140 2.2. Biological data

141 Presence data were compiled for each of six geodid sponge species *Geodia barretti*, *G.*
142 *macandrewii*, *G. atlantica*, *G. hentscheli*, *G. phlegraei* and *G. parva*, for ostur habitat, and for
143 *P. carpenteri*. All geodid presence data was derived from the same dataset as used in
144 Cárdenas et al. (2013) and recovered from the Dryad Repository (<http://www.datadryad.org>)
145 where it is recorded under the Dryad package identifier:
146 <http://dx.doi.org/10.5061/dryad.td8sb>. Ostur presence data was compiled from experts
147 identifications of the habitat (Klitgaard et al., 2001, Klitgaard and Tendal 2004), unpublished
148 sample data held by Plymouth University and data from the NAFO NEREIDA research
149 programme which receives support from EU, Canada, Spain, UK, Russia, Portugal. Ostur
150 presence in the NEREIDA dataset was determined based on agglomerative clustering with
151 average linkage on a subset of data records, with abundance values for selected VME
152 indicator species. A group dominated by a high biomass of geodids was identified as ostur.
153 *P. carpenteri* presence records were those used in Ross and Howell (2013) with additional
154 data compiled from various literature sources (Table 1).

155 In order to control for sample bias in the model (Phillips and Dudík 2008) a background
156 dataset was compiled from all presence data and ‘apparent absence’ data. ‘Apparent
157 absence’ data was determined as trawling or video samples taken within the study area
158 where the target species was not recorded as present. Trawl net mouth openings and video
159 fields of view are at best a few meters wide. We therefore felt that absence data could not be
160 considered reliable when used with environmental data cells of size 1km by 1km resolution.
161 The existence of potential false absences within our dataset, a problem referred to as
162 “imperfect detection” in (Lahoz-Monfort et al., 2014), means that rather than estimating
163 where species occur, we are only able to estimate where they are detected, an inherent
164 limitation of the models. Apparent absence data were compiled from various literature
165 sources and our own data holdings from 222 biological video and photographic transects.
166 Details of all data used in the models are provided in Table 1.

167 2.3. Environmental layers

168 Environmental variables were selected based on their biological relevance, resolution and
169 availability. 16 variables were trialled with preliminary models (Table 2).

170 Bathymetric data were obtained from the General Bathymetric Chart of the Oceans (GEBCO)
171 2008 (<http://www.gebco.net/>) 30 arc second grid, as derived from quality controlled ship
172 soundings combined with satellite-derived gravity data. This dataset provides universal
173 coverage of the study area. The GEBCO bathymetry layer was reprojected into Goode's
174 Homolosine (Ocean) at 1km x 1km grid cell size (the approximate size of cells over the study
175 area) and seven further topographic variables were derived from the bathymetry layer. Slope,
176 curvature, plan curvature, and profile curvature were created using the ArcGIS (ESRI 2009)
177 Spatial Analyst extension. Rugosity, broad scale and fine scale bathymetric position index
178 (BPI) were created using the Benthic Terrain Modeller extension (Whiteet al., 2005). BPI
179 broad was calculated with an inner radius of 5 and an outer radius of 20. BPI fine was
180 calculated with an inner radius of 1 and an outer radius of 5. Further information on the
181 specifics of using topographic variables as surrogates is available in existing literature
182 (Kostylev et al., 2005; Wilson et al., 2007; Guinan et al., 2009; ; Ross and Howell 2013).

183 In addition seven oceanographic variables were investigated including bottom temperature,
184 bottom salinity, bottom dissolved oxygen concentration, bottom oxygen saturation rate,
185 bottom phosphate, nitrate, and silicate concentrations. The raw data were downloaded from
186 the NOAA 2009 world ocean atlas (WOA,
187 http://www.nodc.noaa.gov/OC5/WOA09/netcdf_data.html) as an ".ncdf" file and is the
188 average of a given variable for year 2009. Each depth layer was subsampled to create a 3
189 dimensions (latitude*longitude*depth) Random Forest (Breiman 2001) spatial model. The
190 accuracy of the models was evaluated by computing the correlation between extracted and
191 predicted values on a testing set. This model was then trained on the GEBCO grid to obtain
192 a grid of value of the variable at the seabed in each GEBCO cell. The resulting layer is at the
193 GEBCO cell size (30 arc seconds ~ 1km*1km).

194 Finally, Particulate Organic Carbon (POC) at depth was derived from (Lutz et al., 2007).

195 All data layers were reprojected into Goode Homolosine (Ocean) projection and regrided to
196 1km*1km cell size (Table 2)

197

198 3. Modelling

199 3.1. Modelling method

200 Species / habitat sample data were reduced to one data point per cell of environmental data.

201 Using Guillera-Arroita et al's 2015 simple framework that summarizes how interactions

202 between data type and the sampling process (i.e. imperfect detection and sampling bias)

203 determine the quantity that is estimated by a habitat suitability model, we assessed that we

204 were able to model, at best, relative likelihood data using a presence-background approach.

205 While relative likelihoods are not considered appropriate for use in determining area of

206 occupancy (Guillera-Arroita et al., 2015) real world datasets on the scale at which we are

207 modelling very rarely meet the conditions required to achieve probabilities rather than

208 relative likelihoods. Our aim in this paper was to compare relative estimates of extent and

209 distribution (a measure of area of occupancy) rather than provide actual estimates of extent,

210 and thus we feel the use is justified on this occasion.

211 Maximum entropy (MAXENT) modelling is a presence-only modelling technique developed

212 by (Phillips et al., 2004; Phillips et al., 2006; Phillips and Dudík 2008). It has been found to be

213 amongst the highest performing modelling techniques for presence only modelling (Elith et al.,

214 2006) and as such was selected for use in this study. Presence and apparent absence data

215 points in ArcGIS[®] were overlaid with accompanying environmental variables and the data

216 extracted for use in MAXENT using the Marine Geospatial Ecology Tools add-on (Robertson

217 et al., 2010) . Pre-selection of significant variables was undertaken through preliminary

218 MAXENT runs using the samples-with-data (SWD) approach, with background data

219 comprising all presence and apparent absence data supplied in the same format.

220 Highly correlated variables were identified and the most ecologically relevant correlate and /
221 or most significant in terms of preliminary model gain assessed from jack-knife plots was
222 retained (see supplementary material – Table 1 in Supplementary material for details on
223 correlations). The final variables selected for use in each model are given in Table 2, and the
224 summary statistics of each given in Supplementary material - Table 2).

225 Each model was fitted in R with the 'dismo' package version 0.8-11 (Hijmans et al., 2012)
226 using the MAXENT Java program version 3.3.3k (Phillips and Dudík 2008). Regularization
227 settings were adjusted to reduce overfitting (Phillips and Dudík 2008) resulting in a
228 regularization parameter of 2 for ostur habitat, *G.atlantica*, *G.hentscheli* *G.macandrewii*,
229 *G.parva* and *G.phlegraei* and 3 for *G.barretti* and *P.carpenteri* models. Each model was then
230 projected onto the environmental GIS layers covering the entire study area. Predictions were
231 constrained to sampled conditions using a mask in ArcGIS derived from the MAXENT novel
232 climates output, which highlights combinations in environmental conditions that were not
233 included in the samples used to build the model. MAXENT model output is a logistic
234 probability with values between 0 (low probability) and 1 (high probability). One master
235 model was created for each of the following: ostur habitat, *G.atlantica*, *G.hentscheli*
236 *G.macandrewii*, *G.parva*, *G.phlegraei*, *G.barretti* and *P. carpenteri* .

237

238 3.2. Model evaluation

239 Presence and apparent absence data were used to assess the final models. For each model,
240 100 randomly generated partitions of 75% training/25% test data were used to internally test
241 the model. Discrimination capacity was assessed using the area under the receiver
242 operating curve (AUC). An internal or full model (using all the available data in the training of
243 the model) AUC and a 100 fold cross validation AUC along with training and test average
244 and standard deviation AUCs were calculated. Model assessment and metrics calculation

245 was all done in R using the “dismo” library (Hijmans et al., 2012) and “PresenceAbsence”
246 library (Freeman and Moisen 2008) in R (Team 2011).

247 Although AUC is a widely used statistic in measuring the performance of predictive habitat
248 distribution models, is not without criticism (Lobo et al., 2008; Peterson and Nakazawa 2008;
249 Jiménez-Valverde, 2012) and so the reliability of all models were also assessed using
250 threshold-dependent model evaluation indices (Fielding and Bell 1997).

251 Five thresholding methods recommended by Liu et al., (2005) were considered for each
252 model: sensitivity- specificity equality, sensitivity-specificity sum maximization, ROC-plot-
253 based approaches (Cantor et al., 1999), prevalence, and average probability/suitability
254 approaches (Cramer 2003). The above five methods have a high tolerance to low
255 prevalence training data. Three model performance indices: percent correctly classified
256 (PCC), specificity, and sensitivity (Fielding and Bell 1997; Manel et al., 1999), were
257 calculated for each dichotomised test dataset, resulting from the different thresholding
258 techniques. Index values were then classified on a five-point scale: excellent (1-0.9), good
259 (0.9-0.8), fair (0.8-0.7), poor (0.7-0.6) and fail (0.6-0.5). Considering the averaged threshold-
260 dependent metrics for the partitions together with the same metrics calculated for the full
261 model, a final threshold was chosen to maximize final model performance. Variable
262 importance to a final model was assessed using jack-knife plots (tests comparing model gain
263 for each individual variable in a single variable model, and the reduction in model gain for
264 omitting each variable in turn), as well as the variable response curves.

265

266 3.3. Quantification of habitat distribution

267 MAXENT output probability maps were transferred to ArcGIS as raster grids and masked to
268 restrict prediction to the known range for environmental variables. The maps were then
269 thresholded into predicted presence/absence. Probabilities that fell below the chosen

270 threshold for each species/habitat were converted to a constant absence raster (cell value of
271 0); probabilities above the threshold were retained to later differentiate between areas of
272 high presence probability and low presence probability. A standard deviation of all presence
273 probabilities from 100 partitioned models was also calculated to create a confidence map for
274 each habitat.

275 The distribution of ostur grounds was assessed using 3 maps. The first was produced from
276 the MAXENT model of ostur habitat (hereinafter referred to as the ostur habitat map), the
277 second was produced by combining the six final presence/absence modelled maps for the
278 *geodia* species in a single GIS raster layer indicating the number of geodid sponge species
279 co-occurring in a cell. Where 4 or more species of *geodia* co-occur within a grid cell, the cell
280 was classified as potential ostur presence. This map is hereinafter referred to as the
281 combined geodia map. The third map was produced by overlaying the ostur habitat map with
282 the combined geodia map to produce an ensemble map (hereinafter referred to as the ostur
283 ensemble map).

284

285 3.4. Conservation and management assessment

286 The ArcGIS 10.1 Spatial Analyst extension was used to quantify the areas of predicted
287 presence for both sponge ground types (*ostur* and *P. carpenteri*) within individual nation's
288 EEZs and the High Seas. Additionally predicted area inside existing High Seas MPAs within
289 the study area was calculated. Shapefiles of the boundaries of EEZs and High Seas areas
290 were obtained from <http://www.marineregions.org> and boundaries of the High Seas MPAs
291 as published by Northwest Atlantic Fisheries Organization. The number of presence raster
292 cells within each management division (EEZs and High Seas) was expressed as a
293 percentage of the total number of presence raster cells in the study area. The total number
294 of presence-raster cells within High Seas MPAs is expressed both as a percentage of the

295 total number of presence-raster cells in the study area, and as a percentage of the total
296 number of presence raster cells in the High Seas area.

297

298 4. Results

299 4.1. Modelling

300 Final habitat suitability maps for combined *Geodia*, ostur habitat, ostur ensemble and *P.*
301 *carpenteri* are presented in Fig. 2. Final habitat suitability maps for the individual *Geodia*
302 species are provided in Supplementary material – Figs. 1 to 6.

303

304 4.2. Model evaluation

305 Table 3 displays the AUC values and threshold-dependent model evaluation metrics for all 6
306 *Geodia* models plus the *P. carpenteri* and ostur models. The mean *G. hentscheli* and *G.*
307 *parva* cross-validation AUC scores were considered excellent (0.9-1), while those for *G.*
308 *baretti*, *G. phlegraei*, ostur, and *P. carpenteri* were good (0.8–0.9) and *G. atlantica* and *G.*
309 *macandrewii* fair (0.7–0.8). The Maxent logistic output was thresholded using either minimum
310 ROC distance for *G. barretti*, *G. hentscheli*, *G. macandrewii*, ostur and *P. carpenteri* or
311 Maximum Sensitivity-Specificity for *G. atlantica*, *G. parva* and *G. phlegraei* as shown in
312 Table 3. Models yielded good performances (> 0.8) for *G. hentscheli*, *G. parva*, osturs and *P.*
313 *carpenteri*, fair performances (0.7-0.8) for *G. atlantica*, *G. barretti* and *G. phlegraei* and poor
314 performances (< 0.7) for *G. macandrewii*. The best performing models according to all
315 metrics were *G. hentscheli* and *G. parva*, with *G. atlantica* and *G. macandrewii* performing
316 worst.

317

318 4.3. Assessment of variable importance

319 Jackknife plots identified silicate as the most important variable to the 3 boreal ostur species
320 (*G. barretti*, *G. atlantica* and *G. phlegraei*) and second most important variable to *G.*
321 *macandrewii* in terms of contributing the highest gain when used in isolation. Temperature
322 was the most important variable to the two cold water ostur species *G. hentscheli* and *G.*
323 *parva*, while depth was the most important variable to *P. carpenteri*, *G. macandrewii* and the
324 ostur habitat. Variables that had the most information that wasn't present in the other
325 variables (resulting in the highest decrease in gain when omitted) showed a similar pattern.
326 Silicate was the most important variable to two of the boreal ostur species (*G. atlantica* and
327 *G. phlegraei*) and temperature the most important to *G. barretti*, *G. parva* and *G. hentscheli*,
328 *P. carpenteri* and the ostur habitat. Other important variables included POC for cold water
329 ostur species, ostur habitat and *G. barretti* and depth for *G. atlantica*, *G. phlegraei* and *P.*
330 *carpenteri*. For *G. macandrewii* silicate was also of importance. Jackknife plots and percent
331 contributions of variables to the final models are provided in Supplementary material – Table
332 3.

333

334 4.4. Distribution

335 The model predicts that *P. carpenteri* aggregations are likely to occur on the Mid-Atlantic
336 Ridge (MAR) south of Iceland, on the margin of Greenland and Canada, in the Hatton-
337 Rockall Basin, throughout the Northern Rockall Trough and on the south side of the Faroes-
338 Iceland Ridge, in the Porcupine Seabight, parts of the Bay of Biscay, along the Iberian
339 continental slope and around Galicia Bank, around the Azores, and in most of the western
340 Mediterranean Sea.

341 The distribution of ostur in the combined gGeodia map suggests this habitat is distributed in
342 the Barents Sea, around Svalbard, along the Norwegian shelf, in the Faroe-Shetland
343 Channel, around the Faroes and Iceland, along the Greenland Shelf edge, in the Denmark
344 Strait, on the Flemish Cap, and off the coast of Newfoundland. The distribution suggested by

345 the ostur habitat map is very similar but with notable differences being predictions of
346 presence on the northern Mid Atlantic Ridge, in the Mediterranean, Porcupine Seabight,
347 Rockall-Hatton Plateau and parts of the North Sea, most of which are highly questionable
348 based on our knowledge of these regions. The ostur ensemble map suggests ostur habitat
349 distribution is again similar but more restricted with few presences on the Flemish Cap and
350 on the Mid Atlantic Ridge, and very few off the coast of Newfoundland.

351

352 4.5. Conservation and management assessment

353 The majority of both types of deep-sea sponge habitats are likely to occur inside nations
354 EEZs (Table 4). Assessed from the combined *Geodia* map and the ostur ensemble map, the
355 top five territories with the highest percentage of ostur habitat within their EEZs are Norway,
356 Svalbard, Iceland, Greenland and Canada, although the order varies between models.
357 These same territories are in the top seven (with the addition of the United Kingdom and
358 Ireland) when assessed using the ostur habitat map. . The top five territories with the highest
359 percentage of the *P. carpenteri* habitat resource within their EEZs are Iceland, Italy, Spain,
360 Azores (Portugal) and the UK.

361 For both sponge habitats there are some areas of suitable habitat in the High Seas (Table 5).
362 The current High Seas MPA network contains 13.5% of the High Seas *P. carpenteri*
363 resource (2.9% of the total resource) and between 1.5-19.5% of the High Seas ostur
364 resource (up to 1.5% of the total resource in the ostur habitat map but only 0.07% in the
365 ostur ensemble map).

366

367 5. Discussion

368 5.1. *What environmental factors drive the broad-scale distribution of ostur and*
369 *Pheronema carpenteri sponge grounds?*

370 To three of the geodid species silicate was the most important explanatory variable and is in
371 the top five most important variables for all models. Dissolved silicate is needed by all
372 sponges that have siliceous spicules. This includes glass sponges (Class Hexactinellida)
373 and demosponges (Class Demospongiae). Silicate uptake is an energy demanding process
374 (Frøhlich and Barthel 1997) that is genetically controlled and regulated by silicate
375 concentrations (Krasko et al., 2000). At low concentrations, enzymes needed for spicule
376 formation are not expressed, whereas these enzymes are strongly activated by 60 μM Si.
377 Studies of silicic acid uptake by temperate sublittoral sponges have found that significant
378 uptake rates occur only at silicic acid concentrations higher than those naturally occurring in
379 the sponge habitat, suggesting that these sponge populations are chronically limited by Si
380 availability (Maldonado et al., 2005; Maldonado et al., 2011). If populations are limited by
381 silicate availability it is likely that silicate levels could play an important role in determining
382 geodid sponge habitat distribution.

383 *G. barretti* has been recorded and / or cultivated at silicate levels ranging from 2.79-4.6 μM
384 (Hoffmann et al., 2003). In our study *G. barretti* presence was recorded over a Si range of
385 5.41-24.74 μM (mean 10.52 μM , standard deviation 5.7) (Supplementary material - Table 3).
386 Silicate appeared relatively less important to *P. carpenteri* aggregations, which was
387 unexpected. The occurrence of glass sponge reefs in the relatively shallow waters around
388 British Columbia in the Pacific are thought to be related to the relatively high silicate levels
389 observed there, which do not occur at shelf depths elsewhere (Whitney et al., 2005). Silicate
390 levels observed near these reefs were in the region of 43–75 μM , while In the data set used
391 in this study, the average level of silicate is 17 μM (and 15 for *P. carpenteri* specifically with
392 a maximum of 22). In the Antarctic, siliceous sponges habitat has even higher silicate levels
393 than British Columbia coastal waters, with shelf concentrations exceeding 80 μM (Whitney et
394 al., 2005).

395 It must be noted that silicate was correlated with nitrate, phosphate and depth. Nitrate and
396 phosphate were removed from the final model but we cannot be certain which of the

397 correlated variables is the driving factor. Many sponge species are capable of nitrogen
398 fixation, and (Yahelet al., 2007) observed no significant concentration shift for nitrate
399 between inhalant and exhalent water for 2 deep water species of glass-sponges. Therefore it
400 is less likely that nitrate is a limiting factor. Available research also suggests uptake of
401 phosphate by sponges is negligible and for some species a significantly higher concentration
402 of phosphate has been observed in the exhalent current compared to the inhalant current
403 (Yahel et al., 2007); Perea-Blazquez et al., 2012). Therefore it is again unlikely that
404 phosphate is a limiting factor in sponge distribution. Depth acts as a surrogate for a number
405 of environmental variables with which it is usually correlated including temperature (where
406 biogeography is taken into account), current speed, water mass structure, food availability
407 and sediment type (Howell et al., 2002; Howell, 2010). While in this study neither
408 temperature nor POC were overly correlated with depth, no data were available to us on
409 current speed and sediment type, therefore it is possible and likely that these variables are
410 also important drivers of sponge habitat distribution (see below).

411 Temperature was the most important explanatory variable for the cold water geodid species
412 *G. hentscheli* and *G. parva*. *ostur* habitat has been recorded over a temperature range of -
413 0.5 to 8°C and a narrow salinity range of 34.8-35.5 ppt (Klitgaard and Tendal 2004; Bett
414 2012; Murillo et al., 2012). The cold-water species *G. hentscheli* and *G. parva* have,
415 however, been found over a narrower temperature range of -1.76°C in eastern Greenland to
416 4.5°C west of Iceland and Reykjanes Ridge (Cárdenas et al., 2013). The observations
417 included in this study had a mean temperature of 1.71°C and standard deviation of 1.35
418 (Supplementary material – Table 2). Although there are no data on an upper or lower
419 physiological limit to either of these species it is likely they cannot tolerate temperatures as
420 high as boreal geodid species like *G. barretti*. Therefore, it is highly likely that temperature
421 limits the distribution of both *G. hentscheli* and *G. parva* within the modelled area.

422 In this study *G. barretti* was found over a temperature range of -0.62 to 10.75°C (mean
423 3.22 °C, standard deviation 1.45). While the boreal species can tolerate rapid temperature

424 changes of up to 7°C (Bett, 2012) a recent temperature shock event that occurred on the sill
425 of the Kosterfjord in both 2006 and 2008 is thought to have resulted in a mass mortality in *G.*
426 *barretti*. Temperature increased by approximately 4°C in a 24 hour period on both occasions
427 to over 12°C. The coincidence of the temperature shock events with mass mortality in the
428 species suggested an exceedance of the sponge's physiological limits, although the direct
429 cause of the mortality is not known (Guihenet et al., 2012).

430 Temperature was also an important variable for *P. carpenteri*. Although there are no existing
431 data on the temperature tolerance of *P. carpenteri*, this species is found over a temperature
432 range of 2.73 to 20.9 °C (mean 5.17 °C, standard deviation 2.03) in this study.

433 Depth was the most important variable to the *P. carpenteri* model. As stated previously
434 depth provides a proxy for multiple other variables including current speed and sediment
435 type, which were not considered in this study (Howell et al., 2002; Howell, 2010). Sediment
436 in the water column is important as sponges, being non selective filter feeders, can get
437 clogged if concentration gets too high (Tjensvollet et al., 2013).

438 Current speed, or rather hydrography, is also thought to play an important role in driving the
439 distribution of both ostur and *P. carpenteri* sponge habitat. (Klitgaard et al., 1997; Klitgaard et
440 al., 2001) extended the theories of Frederiksen et al. (1992) to explain the distribution of
441 ostur and Rice et al. (1990) proposed a similar explanation for the distribution of *P.*
442 *carpenteri*. Accumulations of large suspension feeders show a tendency to aggregate near
443 the shelf break in regions with a critical slope where the bottom slope matches the slope of
444 propagation of internal tidal waves. The causal link is thought to be an increase in the supply
445 of food related to the incidence of internal waves which results in resuspension of particulate
446 organic matter on which the sponges feed. While recent studies support these ideas to a
447 degree, they have suggested the forcing mechanism is not necessarily internal tides (White
448 et al., 2003, Hosegood and van Haren 2004; Whitney et al., 2005). White et al. (2003)
449 suggested there is some process that has a daily period and is driven by perturbations of the

450 density gradient that is responsible for generating the oceanographic conditions suitable for
451 *P. carpenteri* sponge ground formation within the Porcupine Seabight. These might be
452 associated with diurnal tidal constituents, inertial oscillations or some other process.

453 POC flux to the seabed was also an important explanatory variable for *P. carpenteri*, the cold
454 water ostur species, *G. barretti*, and to a lesser degree for ostur habitat. Demosponges are
455 generally regarded as unselective suspension feeders, filtering particles from bacterial size
456 to about 6 µm in diameter (Reiswig 1975; Wolfrath and Barthel 1989) and recent studies of
457 two deep water species of hexactinellid sponges has indicated that both species rely largely
458 on free-living, non-photosynthetic bacteria and nano-planktonic protists for nutrition (Yahel et
459 al., 2007). Therefore amount of POC is likely to be a driving factor in determining the
460 distribution of sponge grounds. However, recent research has demonstrated that *G. barretti*
461 is a high microbial abundance (HMA) sponge (Weisz et al., 2008; Hoffmann et al., 2009;).
462 HMA sponges species may potentially use a higher proportion of the total pool of organic
463 matter in seawater, making use of both POC, and DOC via their bacterial symbionts (Weisz
464 et al., 2008). No continuous DOC bottom information was available in the North Atlantic and
465 therefore, DOC was not considered in this study.

466

467 5.2. *What is the predicted distribution of sponge grounds in the northern North Atlantic,*
468 *Norwegian and Barents Sea?*

469 Both the combined *Geodia* and ostur habitat maps suggested similar broad-scale
470 distributions of ostur in the core areas of the Western Barents Sea, Norwegian Shelf, Faroe-
471 Shetland Channel, around the Faroes and Iceland, in the Denmark Strait, then following the
472 continental slope around the tip of Greenland, Labrador Basin, and down to the Flemish Cap.
473 This distribution shows reasonable agreement with the known distribution of the habitat
474 (Klitgaard and Tendal 2004), however, only the ostur habitat model predicts presence on the
475 Mid Atlantic Ridge south of Iceland where ostur have been observed (Klitgaard and Tendal

476 2004). This model also predicts presence on Porcupine Bank, Rockall Bank, Hatton Bank
477 and in the shallow western parts of the North Sea all of which are highly questionable given
478 the level of past sampling in these areas with no recorded presence of ostur habitat.

479 There is also reasonable agreement between these two models and previously published
480 regional models and their input data. Knudby et al. (2013) observed ostur habitat presence
481 around the slopes of the Flemish Cap, along the edge of the Grand Banks, on the shelf from
482 Cumberland Sound and north toward Baffin Island and on the Canadian shelf edge near the
483 Davis Strait, which both models predict albeit in slightly different locations but with some
484 overlap. Knudby et al. (2013) also observed ostur habitat presence along the shelf edge
485 from Newfoundland to Resolution Island. While the ostur habitat map suggests presence
486 here, the combined Geodia model does not.

487 In addition neither model predicts presence on Banquereau Bank where Knudby et al. (2013)
488 observed ostur presence, even though the ostur habitat model predicts their presence on the
489 slope of the bank. The models also failed to predict the presence of osturs at the depth band
490 observed by Bett (2012) in the Faroe-Shetland Channel . Failure of one or both models to
491 predict presence where it has been observed suggests deficiencies in the models. Both the
492 combined Geodia and ostur habitat maps suggest presence on the Canadian Atlantic shelf
493 where Knudby et al. (2013) observed absence. It is possible that absence may be a result of
494 fishing activities as suggested by Knudby et al. (2013) for observed absence on parts of the
495 Flemish Cap, or again this may suggest deficiencies in the models.

496 Both the Knudby et al. (2013) model and our combined Geodia map suggest presence of
497 ostur at the base of the continental slope and extending onto the seafloor of the deep
498 abyssal plain. This lends further support to Knudby et al. (2013) conclusions that the
499 Newfoundland and Labrador slopes are areas where new sponge grounds are most likely to
500 be found with future sampling efforts. We were unable to model the deeper parts of Baffin

501 Bay as these areas fell outside the range of the environmental envelope sampled, given the
502 environmental variables we used.

503 The predicted distribution of *P. carpenteri* aggregations again broadly follows the known
504 distribution of this habitat. It has been observed from the Mid Atlantic Ridge south of Iceland
505 (Copley et al., 1996), west of the Faroe Islands (Burton 1928), near the Darwin Mounds (Bett
506 et al., 2001), in the Rockall-Hatton Basin (Howell et al., 2014) Porcupine Seabight (Rice et
507 al., 1990), on Goban Spur (Duineveld et al., 1997; Flach et al., 1998; Lavaleye et al., 2002),
508 on Le Danois Bank (García-Alegre et al., 2014) and in the Mediterranean (Vacelet 1961).

509 The model predicts presence at all these locations suggesting a reasonable performance.

510 The model shows broad agreement with previously published finer scale models of *P.*
511 *carpenteri* distribution from the UK and Irish extended continental shelf limits (Ross and
512 Howell 2013; Ross et al., 2015). Both the current model and fine scale model of (Ross et al.,
513 2015) predict presence in a narrow band all along the continental slope and in the Porcupine
514 Seabight in this region, where as the (Ross and Howell 2013) model predicted a more
515 patchy distribution for these areas.

516 A regional model of Le Danois Bank off the northern Spanish coast indicated high probability
517 of suitable habitat on the southern and western sides of the bank (García-Alegre et al., 2014)
518 showing good agreement with the current model predictions. Observed presences used in
519 the Le Danois Bank model were all from this area but were not used in the building of the
520 current model again providing encouraging results for the broad-scale model performance.

521 Our model suggests new potentially large areas of presence of *P. carpenteri* sponge habitat
522 may occur in the south eastern corner of the Bay of Biscay offshore from Bilbao and
523 Bordeaux, areas around Galicia Bank, areas flanking the Nazaré and Setúbal Canyons,
524 large parts of the western Mediterranean, and also around the Azores. Interestingly our
525 model predicted very little presence in the western North Atlantic, although areas of the
526 continental slope off-shore of Boston (and at the southern limit of the model) were identified.

527

528 5.3. *Implications for conservation and management*

529 Our results suggest that for both deep-sea sponge aggregations the bulk of the suitable
530 habitat lays inside countries EEZs. 78.7% of *P. carpenteri* deep-sea sponge aggregations
531 and 92-96% of ostur habitat are likely to occur inside EEZs, therefore the effective
532 conservation and management of these habitats will depend on good integration and
533 communication between nations. Responsibility for the designation of marine protected
534 areas and management of most activities that interact with the seabed within EEZs lies at a
535 national level. Thus the development of an ecologically coherent, well managed network of
536 MPAs for the protection of deep-sea sponge aggregations will require those nations with
537 considerable sponge resource (here considered as the top 5 nations in terms of modelled
538 suitable habitat area), such as Iceland, Greenland and Faroes (Denmark), Norway (coastal
539 Norway and Svalbard), Portugal and the UK to engage with the process. Fishing activities
540 are unique in that management tends to operate at a regional level through Regional
541 Fisheries Management Organisations and thus there are opportunities for a more
542 coordinated approach to the management of fishing activities for the conservation of deep-
543 sea sponge habitat. Given the likely occurrence of these habitats, as predicted by our
544 models, within its EEZ, we recommend that the European Commission considers further
545 investigation of these areas and use of the precautionary principle as part of a risk based
546 approach to manage human pressures impacting the deep sea environment.

547 For the small percentage of ostur habitat that is likely to lay in High Seas waters much of this
548 occurs on the Mid Atlantic Ridge (MAR), in the Irminger Basin, on the Flemish Cap and in
549 the Greenland Sea and Norwegian Basin. For both the MAR and Flemish Cap areas the
550 North Atlantic Regional Management Fisheries Organisations (NEAFC and NAFO) have
551 established fishery closures to bottom trawl fishing to protect Vulnerable Marine Ecosystems
552 (VME) in part fulfilment of UNGA Resolution 61/105 for deep-sea sponge aggregations

553 protecting 8-15% of the likely resource. However species and habitats require effective
554 protection measures throughout their range (Green et al., 2014) thus we suggest the High
555 Seas area of the Norwegian and Greenland Seas, predicted by our model as likely to
556 support ostur deep-sea sponge aggregations, are investigated for the presence of ostur
557 habitat and, if observed, consideration given to protection of the seabed habitat in this region.
558 For the 21.3% of *P. carpenteri* deep-sea sponge aggregations that are predicted to occur in
559 High Seas areas much of this occurs on the MAR south of Iceland and in and around the
560 Rockall-Hatton Plateaux including Edoras Bank. While 13.5 % of the High Seas area likely to
561 support *P. carpenteri* aggregations is contained within the existing MPA network (shown in
562 Fig. 1), in the case of the Hatton-Rockall Plateau this is incidental capture as these area
563 closures were made for the protection of cold water corals. The Rockall-Hatton Basin
564 represents a large area where our models predict *P. carpenteri* aggregations are likely to
565 occur. The importance of the Hatton-Rockall Plateaux in this region was recently highlighted
566 by the area being proposed as an 'Ecologically and Biologically Significant Area' (EBSA) to
567 the Convention on Biological Diversity. Human activities occurring in the basin include
568 bottom trawling (likely to only extend to the base of Rockall Bank) and the presence of
569 submarine cables (Benn et al., 2010). We suggest, given the existing observations of
570 presence of this habitat and the likely occurrence of the habitat on the basis of our model
571 output, that areas not previously subjected to bottom trawling are considered for protection
572 by NEAFC and the Irish and UK Governments.

573

574 6. Conclusions

575 Silicate concentration and temperature appear to be the most important drivers for geodid
576 species distribution and depth is the most important for *P. carpenteri*. Depth is, however,
577 most likely acting as a proxy for several unmeasured oceanographic parameters that
578 correlate with depth. POC is also an important predictor for some geodids and *P. carpenteri*.

579 Predicted sponges distribution broadly agrees with previously published distribution maps.
580 Sponge grounds are mainly found at the base of the continental slope and nearby deep
581 seafloor. As most of the sponge aggregation habitat is within EEZs, conservation efforts will
582 need to be coordinated between nations to achieve comprehensive coverage of protected
583 areas. The precautionary principle should be applied to ensure human impact on these
584 species and habitats is limited before a conservation strategy has been designed and
585 implemented. Given how partial the current knowledge of deep-sea sponge ground
586 distribution is, more research should be directed towards determining their extent and
587 distribution through ground-truthing models. In addition research is needed to understand
588 their ecological requirements, and how they are impacted by human activities in order to
589 predict their response in a changing environment.

590

591 7. Acknowledgements

592 We are grateful to P. Cárdenas and all those who donated data to his study of *Geodia*
593 species in the Atlantic boreo-arctic region. We are also grateful to the NAFO NEREIDA
594 research programme which receives support from EU, Canada, Spain, UK, Russia, and
595 Portugal. This study was funded by The UK's Department for Environment, Food & Rural
596 Affairs under project MF1006, and a Santander scholarship awarded to KLH.

597

598 8. References

599 Bell, J.J. 2008. The functional roles of marine sponges. - *Estuar Coast Shelf S.* 79, 341-353.

600

601 Benn, A.R., Weaver, P.P., Billet, D.S., Van Den Hove, S., Murdock, A.P., Doneghan, G.B.
602 and Le Bas, T. 2010. Human activities on the deep seafloor in the North East Atlantic: an
603 assessment of spatial extent. - *PLoS ONE* 5: e12730.

604
605
606
607
608
609
610
611
612
613
614
615
616
617
618
619
620
621
622
623
624
625
626
627
628
629
630

Bett, B., Billett, D., Masson, D. and Tyler, P. 2001. RRS Discovery cruise 248. A multidisciplinary study of the environment and ecology of deep-water coral ecosystems and associated seabed facies and features (The Darwin Mounds, Porcupine Bank and Porcupine Seabight). - Cruise report 36: 52.

Bett, B.J. and Rice, A.L. 1992. The influence of hexactinellid sponge (*Pheronema carpenteri*) spicules on the patchy distribution of macrobenthos in the porcupine seabight (bathyal NE Atlantic). - Ophelia 36, 217-226.

Bett, B.J., 2012, Seafloor biotope analysis of the deep waters of the SEA4 region of Scotland's seas, JNCC Report 472, A4, 99pp.

Bowerbank, J.S. 1858. On the anatomy and physiology of the Spongiadae. - Philos. Trans. R. Soc. London 148: 279-332.

Breiman, L. 2001. Random forests. - Mach. Learn. 45, 5-32.

Burton, M. 1928. Hexactinellida. Danish Ingolf Expedition 6(4): 1-18..

Cantor, S.B., Sun, C.C., Tortolero-Luna, G., Richards-Kortum, R. and Follen, M. 1999. A comparison of C/B ratios from studies using receiver operating characteristic curve analysis. - J. Chronic Dis. 52, 885-892.

Cárdenas, P., Rapp, H.T., Schander, C. and Tendal, O.S. 2010. Molecular taxonomy and phylogeny of the Geodiidae (Porifera, Demospongiae, Astrophorida)–combining phylogenetic and Linnaean classification. Zool. Scr. 39, 89-106.

631 Cárdenas, P., Rapp, H.T., Klitgaard, A.B., Best, M., Thollesson, M. and Tendal, O.S. 2013.
632 Taxonomy, biogeography and DNA barcodes of *Geodia* species (Porifera, Demospongiae,
633 Tetractinellida) in the Atlantic boreo - arctic region. *J. Linn. Soc. London, Zool.* 169, 251-311.
634
635 Cathalot, C., Van Oevelen, D., Cox, T., Kutti, T., Lavaleye, M., Duineveld, G. and Meysman,
636 F. J. 2015. Cold-water coral reefs and adjacent sponge grounds: Hotspots of benthic
637 respiration and organic carbon cycling in the deep sea. *Front. Mar. Sci.* 2, 37.
638
639 Copley, J., Tyler, P., Shearer, M., Murton, B. and German, C. 1996. Megafauna from
640 sublittoral to abyssal depths along the Mid-Atlantic Ridge south of Iceland. *Oceanol. Acta* 19,
641 549-559.
642
643 Cramer, J.S. 2003. Logit models from economics and other fields. Cambridge University
644 Press.
645
646 Dambach, J. and Rodder, D. 2011. Applications and future challenges in marine species
647 distribution modeling. *Aquat. Conserv.* 21, 92-100.
648
649 Davies, A.J., Wisshak, M., Orr, J.C. and Roberts, J.M. 2008. Predicting suitable habitat for
650 the cold-water coral *Lophelia pertusa* (Scleractinia). *Deep Sea Res., Part I* 55, 1048-1062.
651
652 Degraer, S., Verfaillie, E., Willems, W., Adriaens, E., Vincx, M. and Van Lancker, V. 2008.
653 Habitat suitability modelling as a mapping tool for macrobenthic communities: an example
654 from the Belgian part of the North Sea. *Cont. Shelf Res.* 28, 369-379.
655

656 Dolan, M.F.J., Grehan, A.J., Guinan, J.C. and Brown, C. 2008. Modelling the distribution of
657 cold-water corals in relation to bathymetric variables: adding spatial contact to deep-sea
658 video. *Deep-Sea Res. Part 1*, 1564-1579.

659

660 Duineveld, G., Lavaleye, M., Berghuis, E., De Wilde, P., Van Der Weele, J., Kok, A., Batten,
661 S. and De Leeuw, J. 1997. Patterns of benthic fauna and benthic respiration on the Celtic
662 continental margin in relation to the distribution of phytodetritus. *Int. Rev. Gesamten*
663 *Hydrobiol. Hydrogr.* 82, 395-424.

664

665 Elith, J., Graham, C.H., Anderson, R.P., Dudik, M., Ferrier, S., Guisan, A., Hijmans, R.J.,
666 Huettmann, F., Leathwick, J.R., Lehmann, A., Li, J., Lohmann, L.G., Loiselle, B.A., Manion,
667 G., Moritz, C., Nakamura, M., Nakazawa, Y., Overton, J.M., Peterson, A.T., Phillips, S.J.,
668 Richardson, K., Scachetti-Pereira, R., Schapire, R.E., Soberon, J., Williams, S., Wisz, M.S.
669 and Zimmermann, N.E. 2006. Novel methods improve prediction of species' distributions
670 from occurrence data. *Ecography* 29, 129-151.

671

672 Elith, J. and Leathwick, J.R. 2009. Species Distribution Models: Ecological Explanation and
673 Prediction Across Space and Time. In: *Annual Review of Ecology Evolution and Systematics*.
674 *Annual Reviews*, pp. 677-697.

675

676

677 Ferrier, S. and Guisan, A. 2006. Spatial modelling of biodiversity at the community level. *J.*
678 *Appl. Ecol.* 43, 393-404.

679

680 Fielding, A.H. and Bell, J.F. 1997. A review of methods for the assessment of prediction
681 errors in conservation presence/absence models. *Environ. Conserv.* 24, 38-49.

682

683 Flach, E., Lavaleye, M., De Stigter, H. and Thomsen, L. 1998. Feeding types of the benthic
684 community and particle transport across the slope of the NW European continental margin
685 (Goban Spur). Prog. Oceanogr. 42, 209-231.
686

687 Frederiksen, R., Jensen, A. and Westerberg, H. 1992. The distribution of the scleractinian
688 coral *Lophelia pertusa* around the Faroe Islands and the relation to internal tidal mixing.
689 Sarsia 77, 157-171.
690

691 Freeman, E.A. and Moisen, G. 2008. Presence Absence: An R package for presence
692 absence analysis. J. Stat. Softw. 23, 1-31.
693

694 Frøhlich, H. and Barthel, D. 1997. Silica uptake of the marine sponge *Halichondria panicea*
695 in Kiel Bight. Mar. Biol. 128, 115-125.
696

697 Galparsoro, I., Borja, A., Bald, J., Liria, P. and Chust, G. 2009. Predicting suitable habitat for
698 the European lobster (*Homarus gammarus*), on the Basque continental shelf (Bay of Biscay),
699 using Ecological-Niche Factor Analysis. Ecol. Modell. 220, 556-567.
700

701 García-Alegre, A., Sánchez, F., Gómez-Ballesteros, M., Hinz, H., Serrano, A. and Parra, S.
702 2014. Modelling and mapping the local distribution of representative species on the Le
703 Danois Bank, El Cachucho Marine Protected Area (Cantabrian Sea). Deep Sea Res., Part II,
704 106, pp.151-164.
705

706 Gonzalez-Mirelis, G. and Lindegarth, M. 2012. Predicting the distribution of out-of-reach
707 biotopes with decision trees in a Swedish marine protected area. Ecol. Appl. 22, 2248-2264.
708

709 Green, A.L., Maypa, A.P., Almany, G.R., Rhodes, K.L., Weeks, R., Abesamis, R.A., Gleason,
710 M.G., Mumby, P.J. and White, A.T. 2014. Larval dispersal and movement patterns of coral
711 reef fishes, and implications for marine reserve network design. *Biol. Rev.* 90, pp.1215-1247..
712

713 Guihen, D., White, M. and Lundälv, T. 2012. Temperature shocks and ecological
714 implications at a cold-water coral reef. *Mar. Biodivers. Rec.* 5: e68.
715

716 Guillera-Aroita, G., Lahoz - Monfort, J.J., Elith, J., Gordon, A., Kujala, H., Lentini, P.E.,
717 McCarthy, M.A., Tingley, R. and Wintle, B.A. 2015. Is my species distribution model fit for
718 purpose? Matching data and models to applications. *Glob. Ecol. Biogeogr.* 24, 276-292.
719

720 Guinan, J., Grehan, A.J., Dolan, M.F.J. and Brown, C. 2009. Quantifying relationships
721 between video observations of cold-water coral cover and seafloor features in Rockall
722 Trough, west of Ireland. *Mar. Ecol. Prog. Ser.* 375, 125-138.
723

724 Hadas, E., Marie, D., Shpigel, M. and Ilan, M. 2006. Virus predation by sponges is a new
725 nutrient-flow pathway in coral reef food webs. *Limnol. Oceanogr.* 51, 1548-1550.
726

727 Hansen, G.A. 1885. Spongiadae. The Norwegian North-Atlantic Expedition 1876–1878.
728 *Zoology* 13, 1-26.
729

730 Hijmans, R.J., Phillips, S., Leathwick, J., Elith, J. and Hijmans, M.R.J. 2012. Package ‘dismo’
731 *Circles*, 9, p.1..
732

733 Hoffmann, F., Rapp, H.T., Zöller, T. and Reitner, J. 2003. Growth and regeneration in
734 cultivated fragments of the boreal deep water sponge *Geodia barretti* Bowerbank, 1858
735 (Geodiidae, Tetractinellida, Demospongiae) *J. Biotechnol.* 100, 109-118.

736

737 Hoffmann, F., Radax, R., Woebken, D., Holtappels, M., Lavik, G., Rapp, H.T., Schläppy, M.
738 L., Schleper, C. and Kuypers, M.M. 2009. Complex nitrogen cycling in the sponge *Geodia*
739 *barretti*. Environ microbiol 11, 2228-2243.

740

741 Hosegood, P. and van Haren, H. 2004. Near-bed solibores over the continental slope in the
742 Faeroe-Shetland Channel. Deep Sea Res., Part II 51, 2943-2971.

743

744 Howell, K., Huvenne, V., Piechaud, N., Robert, K. and Ross, R. 2013. Analysis of biological
745 data from the JC060 survey of areas of conservation interest in deep waters off north and
746 west Scotland. JNCC Report No. 528..

747

748 Howell, K.L., Billett, D.S. and Tyler, P.A. 2002. Depth-related distribution and abundance of
749 seastars (Echinodermata: Asteroidea) in the Porcupine Seabight and Porcupine Abyssal
750 Plain, NE Atlantic. Deep Sea Res., Part I 49, 1901-1920.

751

752 Howell, K.L. 2010. A benthic classification system to aid in the implementation of marine
753 protected area networks in the deep/high seas of the NE Atlantic. Biol. Cons. 143, 1041-
754 1056.

755

756 Howell, K.L., Holt, R., Endrino, I.P. and Stewart, H. 2011. When the species is also a habitat:
757 Comparing the predictively modelled distributions of *Lophelia pertusa* and the reef habitat it
758 forms. Biol. Cons. 144, 2656-2665.

759

760 Hughes, D.J. and Gage, J.D. 2004. Benthic metazoan biomass, community structure and
761 bioturbation at three contrasting deep-water sites on the northwest European continental
762 margin. Prog. Oceanogr. 63, 29-55.

763

764 Jiménez-Valverde, A. 2012. Insights into the area under the receiver operating characteristic
765 curve (AUC) as a discrimination measure in species distribution modelling. *Glob. Ecol.*
766 *Biogeogr.* 21, 498-507.

767

768 Kenchington, R. and Hutchings, P. 2012. Science, biodiversity and Australian management
769 of marine ecosystems. *Ocean Coast. Manage.* 69, pp.194-199.

770

771 Klitgaard, A.B., Tendal, O.S. and Westerberg, H. 1997. Mass occurrences of large sponges
772 (Porifera) in Faroe Island (NE Atlantic) shelf and slope areas: characteristics, distribution and
773 possible causes. In: *Proceedings of the 30th European Marine Biological Symposium*,
774 Southampton, UK, 5. pp. 129-142.

775

776 Klitgaard, A.B. and Tendal, O.S. 2001. "Ostur"- "Cheese Bottoms"-sponge dominated areas
777 in the Faroese shelf and slope areas. In: Bruntse G, Tendal O.S. (Eds.) *Marine Biological*
778 *Investigations and Assemblages of Benthic Invertebrates From the Faroese Islands*. Kaldbak
779 Marine Biological Laboratory, Faroe Islands, pp13-21.

780

781 Klitgaard, A.B. and Tendal, O.S. 2004. Distribution and species composition of mass
782 occurrences of large-sized sponges in the northeast Atlantic. *Prog. Oceanogr.* 61, 57-98.

783

784 Knudby, A., Kenchington, E. and Murillo, F.J. 2013. Modeling the distribution of geodia
785 sponges and sponge grounds in the northwest atlantic. *PloS ONE* 8: e82306.

786

787 Kostylev, V.E., Erlandsson, J., Ming, M.Y. and Williams, G.A. 2005. The relative importance
788 of habitat complexity and surface area in assessing biodiversity: fractal application on rocky
789 shores. *Ecol. Complex.* 2, 272-286.

790

791 Krasko, A., Lorenz, B., Batel, R., Schröder, H.C., Müller, I.M. and Müller, W.E. 2000.
792 Expression of silicatein and collagen genes in the marine sponge *Suberites domuncula* is
793 controlled by silicate and myotrophin. Eur. J. Biochem. 267, 4878-4887.
794

795 Lahoz-Monfort, J.J., Guillera-Arroita, G. and Wintle, B.A. 2014. Imperfect detection impacts
796 the performance of species distribution models. Glob. Ecol. Biogeogr. 23, 504-515.
797

798 Lavaleye, M., Duineveld, G., Berghuis, E., Kok, A. and Witbaard, R. 2002. A comparison
799 between the megafauna communities on the NW Iberian and Celtic continental margins—
800 effects of coastal upwelling? Prog. Oceanogr. 52, 459-476.
801

802 Liu, C., Berry, P.M., Dawson, T.P. and Pearson, R.G. 2005. Selecting thresholds of
803 occurrence in the prediction of species distributions. Ecography 28, 385-393.
804

805 Lobo, J.M., Jiménez-Valverde, A. and Real, R. 2008. AUC: a misleading measure of the
806 performance of predictive distribution models. Glob. Ecol. Biogeogr. 17, 145-151.
807

808 Lutz, M.J., Caldeira, K., Dunbar, R.B. and Behrenfeld, M.J. 2007. Seasonal rhythms of net
809 primary production and particulate organic carbon flux to depth describe the efficiency of
810 biological pump in the global ocean. J Geophys. Res-Oceans 112 (C10),
811

812 Maldonado, M., Carmona, M.C., Velásquez, Z., Puig, A., Cruzado, A., López, A. and Young,
813 C.M. 2005. Siliceous sponges as a silicon sink: an overlooked aspect of benthopelagic
814 coupling in the marine silicon cycle. Limnol. Oceanogr. 50, 799-809.
815

816 Maldonado, M., Cao, H., Cao, X., Song, Y., Qu, Y. and Zhang, W. 2011. Experimental silicon
817 demand by the sponge *Hymeniacidon perlevis* reveals chronic limitation in field populations.
818 In: Ancient Animals, New Challenges. Springer, pp. 251-257.
819

820 Maldonado, M., Aguilar, R., Bannister, R.J., Bell, D., Conway, K.W., Dayton, P.K., Díaz, C.,
821 Gutt, J., Kenchington, E.L.R., Leys, D. and Pomponi, S.A., 2016. Sponge grounds as key
822 marine habitats: a synthetic review of types, structure, functional roles, and conservation
823 concerns. In: Marine Animal Forests. Springer, Berlin._24-1.

824 Manel, S., Dias, J., Buckton, S. and Ormerod, S. 1999. Alternative methods for predicting
825 species distribution: an illustration with Himalayan river birds. J. Appl. Ecol. 36, 734-747.
826

827 Murillo, F.J., Muñoz, P.D., Cristobo, J., Ríos, P., González, C., Kenchington, E. and Serrano,
828 A. 2012. Deep-sea sponge grounds of the Flemish Cap, Flemish Pass and the Grand Banks
829 of Newfoundland (Northwest Atlantic Ocean): distribution and species composition. Mar. Biol.
830 Res. 8, 842-854.
831

832 Perea-Blazquez, A., Davy, S.K. and Bell, J.J. 2012. Estimates of particulate organic carbon
833 flowing from the pelagic environment to the benthos through sponge assemblages. - PloS
834 ONE 7: e29569.
835

836 Peterson, A. and Nakazawa, Y. 2008. Environmental data sets matter in ecological niche
837 modelling: an example with *Solenopsis invicta* and *Solenopsis richteri*. Glob. Ecol. Biogeogr.
838 17, 135-144.
839

840 Phillips, S.J., Dudík, M. and Schapire, R.E. 2004. A Maximum Entropy Approach to Species
841 Distribution Modeling. In: Proceedings of the 21st International Conference on Machine
842 Learning, Banff, Canada, 2004. ACM Press, New York, pp. 655-662.
843

844 Phillips, S.J., Anderson, R.P. and Schapire, R.E. 2006. Maximum entropy modeling of
845 species geographic distributions. *Ecol. Modell.* 190, 231-259.
846

847 Phillips, S.J. and Dudík, M. 2008. Modelling of Species Distributions with Maxent: New
848 Extensions and a Comprehensive Evaluation. *Ecography* 31, 161-175.
849

850 Piechaud, N., Downie, A., Stewart, H.A. and Howell, K.L. 2015. The impact of modelling
851 method selection on predicted extent and distribution of deep-sea benthic assemblages.
852 *Earth Environ. Sci. Trans. R. Soc. Edinburgh* 105, 251-261.
853

854 Pile, A.J. and Young, C.M. 2006. The natural diet of a hexactinellid sponge: benthic–pelagic
855 coupling in a deep-sea microbial food web. *Deep Sea Res., Part I* 53, 1148-1156.
856

857 Reiswig, H.M. 1971. Particle feeding in natural populations of three marine demosponges. -
858 *Biol. Bull.* 141, 568-591.
859

860 Reiswig, H.M. 1974. Water transport, respiration and energetics of three tropical marine
861 sponges. *J. Exp. Mar. Biol. Ecol.* 14, 231-249.
862

863 Reiswig, H.M. 1975. Bacteria as food for temperate-water marine sponges. *Can. J. Zool.* 53,
864 582-589.
865

866 Rengstorf, A.M., Yesson, C., Brown, C. and Grehan, A.J. 2013. High-resolution habitat
867 suitability modelling can improve conservation of vulnerable marine ecosystems in the deep
868 sea. *J. Biogeogr.* 40, pp.1702-1714.
869

870 Rice, A., Thurston, M. and New, A. 1990. Dense aggregations of a hexactinellid sponge, < i>
871 *Pheronema carpenneri*</i>, in the Porcupine Seabight (northeast Atlantic Ocean), and
872 possible causes. Prog. Oceanogr. 24, 179-196.
873
874 Rice, A.L., Thurston, M.H. and New, A.L. 1990. Dense aggregations of a hexactinellid
875 sponge, *Pheronema carpenneri*, in the Porcupine Seabight (northeast Atlantic Ocean), and
876 possible causes. Prog. Oceanogr. 24, 179-196.
877
878 Rinne, H., Kaskela, A., Downie, A.L., Tolvanen, H., von Numers, M. and Mattila, J. 2014.
879 Predicting the occurrence of rocky reefs in a heterogeneous archipelago area with limited
880 data. Estuar. Coast. Shelf. S. 138, 90-100.
881
882 Roberts, J.J., Best, B.D., Dunn, D.C., Treml, E.A. and Halpin, P.N. 2010. Marine Geospatial
883 Ecology Tools: An integrated framework for ecological geoprocessing with ArcGIS, Python,
884 R, MATLAB, and C++. Environ. Model. Softw 25, 1197-1207.
885
886 Robinson, L.M., Elith, J., Hobday, A.J., Pearson, R.G., Kendall, B.E., Possingham, H.P. and
887 Richardson, A.J. 2011. Pushing the limits in marine species distribution modelling: lessons
888 from the land present challenges and opportunities. Glob. Ecol. Biogeogr. 20, 789-802.
889
890 Rodríguez, E., López-González, P.J. and Gili, J.M. 2007. Biogeography of Antarctic sea
891 anemones (Anthozoa, Actiniaria): What do they tell us about the origin of the Antarctic
892 benthic fauna? Deep Sea Res., Part II 54, 1876-1904.
893
894 Ross, L.K., Ross, R.E., Stewart, H.A. and Howell, K.L. 2015. The Influence of Data
895 Resolution on Predicted Distribution and Estimates of Extent of Current Protection of Three
896 'Listed' Deep-Sea Habitats. PloS ONE 10, e0140061.
897

898 Ross, R.E. and Howell, K.L. 2013. Use of predictive habitat modelling to assess the
899 distribution and extent of the current protection of 'listed' deep-sea habitats. *Diversity and*
900 *Distributions* 19, 433-445.

901

902 Sollas, W. 1880. XVII.—The sponge-fauna of Norway; a report on the Rev. AM Norman's
903 collection of sponges from the Norwegian Coast. *J. Nat. Hist.* 9, 141-165.

904

905 Stephens, J. 1915. *Sponges of the Coasts of Ireland*. H.M. Stationery Office.

906

907 Team, R.D.C. 2011. *R: A Language and Environment for Statistical Computing*. In: R
908 Foundation for Statistical Computing. R Foundation for Statistical Computing, Vienna,
909 Austria.

910

911 Thomson, W. 1869. On *Holtenia*, a Genus of Vitreous Sponges. *Proc. R. Soc. London* 18,
912 32-35.

913 Tjensvoll, I., Kutti, T., Fosså, J.H. and Bannister, R. 2013. Rapid respiratory responses of the
914 deep-water sponge *Geodia barretti* exposed to suspended sediments. *Aquat Biol* 19, 65-73.

915

916 Topsent, E. 1928. *Spongiaires de l'Atlantique et de la Méditerranée, provenant des*
917 *croisières du prince Albert Ier de Monaco*. Imprimerie de Monaco.

918

919 Vacelet, J. 1961. Quelques éponges remarquables de Méditerranée. *Rev. Trav. Inst. Peches*
920 *Marit.* 25, 351-354.

921

922 Weisz, J.B., Lindquist, N. and Martens, C.S. 2008. Do associated microbial abundances
923 impact marine demosponge pumping rates and tissue densities? *Oecol.* 155, 367-376.

924

925 White, M., Mohn, C., de Stigter, H. and Mottram, G. 2003. Deep-water coral development as
926 a function of hydrodynamics and surface productivity around the submarine banks of the
927 Rockall Trough, NE Atlantic. In: 2nd International Symposium on Deep-Sea Corals. pp. 503-
928 514.

929

930 White, M., Mohn, C., de Stigter, H. and Mottram, G. 2005. Deep-water coral development as
931 a function of hydrodynamics and surface productivity around the submarine banks of the
932 Rockall Trough, NE Atlantic. In: Cold-water corals and ecosystems. Springer, pp. 503-514.

933

934 Whitney, F., Conway, K., Thomson, R., Barrie, V., Krautter, M. and Mungov, G. 2005.
935 Oceanographic habitat of sponge reefs on the Western Canadian Continental Shelf. - Cont.
936 Shelf Res. 25, 211-226.

937

938 Wilson, S., Graham, N. and Polunin, N. 2007. Appraisal of visual assessments of habitat
939 complexity and benthic composition on coral reefs. Mar. Biol. 151, 1069-1076.

940

941 Wolfrath, B. and Barthel, D. 1989. Production of faecal pellets by the marine sponge
942 *Halichondria panicea* Pallas (1766). J. Exp. Mar. Biol. Ecol. 129, 81-94.

943

944 Wulff, J.L. 2006. Ecological interactions of marine sponges. Can. J. Zool. 84, 146-166.

945

946 Yahel, G., Sharp, J.H., Marie, D., Hase, C. and Genin, A. 2003. In situ feeding and element
947 removal in the symbiont-bearing sponge *Theonella swinhoei*. Bulk DOC is the major source
948 for carbon. Limnol. Oceanogr. 48, 141-149.

949

950 Yahel, G., Whitney, F., Reiswig, H.M., Eerkes-Medrano, D.I. and Leys, S.P. 2007. In situ
951 feeding and metabolism of glass sponges (Hexactinellida, Porifera) studied in a deep
952 temperate fjord with a remotely operated submersible. Limnol. Oceanogr. 52, 428-440.

953

954

955 Table 1: Number of presence and 'apparent absence' records used in the model for each
 956 species or habitat, including references to the data sources.

Species / habitat	Number of presence	Number of pseudo-absence	References
<i>G. atlantica</i>	60	1714	(Rice et al. 1990, Bett and Rice 1992, Copley et al. 1996, Duineveld et al. 1997, Lavaleye et al. 2002, Klitgaard and Tendal 2004, Gebruk et al. 2010, Howell 2010, Tecchio et al. 2011, Cardenas et al. 2013), NEREIDA; http://www.nafo.int/science/frames/nereida.html), BioICE, http://utgafa.ni.is/greinar/BIOICE_station_list_91-04_Paper_A2.pdf
<i>G. barretti</i>	46	1708	
<i>G. hentscheli</i>	66	1694	
<i>G. macandrewii</i>	148	1648	
<i>G. phlegraei</i>	76	1705	
<i>G. parva</i>	40	1697	
<i>ostur</i>	105	2660	(Klitgaard 1995, Klitgaard and Tendal 2004, Cardenas et al. 2013), NEREIDA; http://www.nafo.int/science/frames/nereida.html), BioICE, http://utgafa.ni.is/greinar/BIOICE_station_list_91-04_Paper_A2.pdf
<i>P. carpenteri</i>	117	1944	(Topsent 1892, Topsent and ler 1904, Stephens and Branch 1915, Burton and Ingolf-Expedition 1928, Topsent 1928, Rice et al. 1990, Bett and Rice 1992, Copley et al. 1996, Duineveld et al. 1997, Lavaleye et al. 2002, Klitgaard and Tendal 2004, Fiore and Jutte 2010, Gebruk et al. 2010, Howell 2010, Tecchio et al. 2011, Cardenas et al. 2013, Narayanaswamy et al. 2013, Vacelet, 1961) , NEREIDA; http://www.nafo.int/science/frames/nereida.html), BioICE, http://utgafa.ni.is/greinar/BIOICE_station_list_91-04_Paper_A2.pdf

957

958

959 Table 2: Summary of the environmental data layers used in this study prior to variable selection. Data sources are given.
 960 Oceanographic variables have been resampled to match the resolution of the GEBCO bathymetry with the method described in the
 961 text.

Variable	units	Manipulation	Original cell size	Source	Used in final models
Terrain variables					
Depth	m	None	0.016°	GEBCO 2008	Y
Slope	-	Created using ArcGIS Spatial Analyst Extension.	0.016°	GEBCO 2008	Y
Curvature	-	Created using ArcGIS Spatial Analyst Extension.	0.016°	GEBCO 2008	Y
Plan curvature	-	Created using ArcGIS Spatial Analyst Extension.	0.016°	GEBCO 2008	N
Profile curvature	-	Created using ArcGIS Spatial Analyst Extension.	0.016°	GEBCO 2008	N
terrain ruggedness	-	Created using ArcGIS Benthic Terrain Modeler extension (Wright et al., 2005).	0.016°	GEBCO 2008	Y
Broad-scale Bathymetric Position Index (BPI)	-	Created using ArcGIS Benthic Terrain Modeler extension (Wright et al., 2005). Inner radius 5, outer radius 20, scale factor is 20 km	0.016°	GEBCO 2008	Y
Fine-Scale Bathymetric Position Index (BPI)	-	Created using ArcGIS Benthic Terrain Modeler extension (Wright et al., 2005). Inner radius 1, outer radius 5, scale factor is 5 km	0.016°	GEBCO 2008	Y
Oceanographic variables					
Bottom temperature	°C	rescaled to 0.016° using random forest modelling	1°	WOA 2009 (Locarnini et al., 2010)	Y
Bottom salinity (PSS)	-	rescaled to 0.016° using random forest modelling	1°	WOA 2009 (Antonov et al., 2010)	Y (except <i>P. carpenteri</i>)

Bottom dissolved oxygen conc.	ml/l	rescaled to 0.016 ⁰ using random forest modelling	1 ⁰	WOA 2009 (Garcia et al., 2010a)	N
Bottom oxygen saturation rate	-	rescaled to 0.016 ⁰ using random forest modelling	1 ⁰	WOA 2009 (Garcia et al., 2010a)	N
Bottom phosphate	µmol/l	rescaled to 0.016 ⁰ using random forest modelling	1 ⁰	WOA 2009 (Garcia et al., 2010b)	N
Bottom nitrate	µmol/l	rescaled to 0.016 ⁰ using random forest modelling	1 ⁰	WOA 2009 (Garcia et al., 2010b)	N
Bottom silicate	µmol/l	rescaled to 0.016 ⁰ using random forest modelling	1 ⁰	WOA 2009 (Garcia et al., 2010b)	Y
Particulate organic carbon flux to seabed	Mg/m ² /year	None	7*7 km	derived from Lutz et al (2007)	Y

962

963

964 Table 3: Summary of each model performance according to Area Under the Curve (AUC) and threshold dependent evaluation including
 965 Percent Correctly Classified (PCC). The full model AUC is the internal AUC of the model trained on the whole dataset. MSS (MaxSens+Spec)
 966 is the threshold value that maximizes the sum of sensitivity and specificity, ROC (MinROCDist) is the threshold values that minimizes the
 967 distance between the Receiver Operating Curve plot and the upper left corner of the unit square.

Species	mean AUC	standard deviation	full model AUC	threshold (method)	PCC	Sensitivity	Specificity
<i>G. atlantica</i>	0.774	0.062	0.865	0.450 (mss)	0.729	0.782	0.727
<i>G. baretti</i>	0.865	0.029	0.876	0.272 (roc)	0.803	0.790	0.805
<i>G. hentscheli</i>	0.942	0.030	0.94	0.238 (roc)	0.930	0.895	0.931
<i>G. macandrewii</i>	0.753	0.043	0.835	0.430 (roc)	0.689	0.743	0.687
<i>G. parva</i>	0.906	0.030	0.928	0.277 (mss)	0.904	0.823	0.907
<i>G. phlegraei</i>	0.826	0.069	0.908	0.448 (mss)	0.825	0.798	0.826
ostur	0.898	0.027	0.881	0.397 (roc)	0.811	0.829	0.810
<i>P. carpenteri</i>	0.891	0.026	0.905	0.372 (roc)	0.805	0.867	0.803

968

969

970 Table 4: Percentage of the extent of suitable habitat predicted that is included within each
 971 nation's Exclusive Economic Zone (EEZ) and the High Seas. The nations listed are ranked
 972 in order of the nations with the highest percentage of ostur within their EEZ according to the
 973 ensemble model. The 'Rank' column provides the equivalent listing for the *P. carpenteri*
 974 model for rapid reading.

Region (Country EEZ or High Seas)	% total area combined Geodia map	% total area ostur habitat map	% total area ostur Ensemble map	% total area <i>P.carpenteri</i>	r a n k s
Greenlandic Exclusive Economic Zone	23.99	39.98	33.47	3.63	
Norwegian Exclusive Economic Zone	16.25	12.13	25.54	0.00	
Icelandic Exclusive Economic Zone	9.06	16.87	14.83	16.29	2
Faeroe Islands Exclusive Economic Zone	6.36	6.39	10.54	2.82	
Canadian Exclusive Economic Zone	13.40	11.51	5.60	1.06	
Svalgaard	2.12	4.84	5.15	0.00	
United Kingdom Exclusive Economic Zone	8.50	2.29	3.74	6.52	6
High Seas	7.94	4.02	0.56	21.30	1
Fisheries Zone around Jan Mayen	0.16	1.86	0.39	0.00	
Portuguese Exclusive Economic Zone (Azores)	2.43	0.10	0.18	9.24	5
Portuguese Exclusive Economic Zone	0.56	0.00	0.00	0.50	
Irish Exclusive Economic Zone	5.50	0.00	0.00	3.09	
Saint-Pierre and Miquelon Exclusive Economic Zone	0.03	0.00	0.00	0.00	
French Exclusive Economic Zone	1.60	0.00	0.00	4.95	7
Spanish Exclusive Economic Zone	1.24	0.00	0.00	13.25	4
United States Exclusive Economic Zone	0.37	0.00	0.00	0.10	
German Exclusive Economic Zone	0.20	0.00	0.00	0.00	
Danish Exclusive Economic Zone	0.14	0.00	0.00	0.00	
Swedish Exclusive Economic Zone	0.06	0.00	0.00	0.00	
Italian Exclusive Economic Zone	0.05	0.00	0.00	13.50	3
Dutch Exclusive Economic Zone	0.02	0.00	0.00	0.00	
Guernsey Exclusive Economic Zone	0.00	0.00	0.00	0.00	
MonUgasque Exclusive Economic Zone	0.00	0.00	0.00	0.01	
Algerian Exclusive Economic Zone	0.00	0.00	0.00	3.18	
Tunisian Exclusive Economic Zone	0.00	0.00	0.00	0.53	

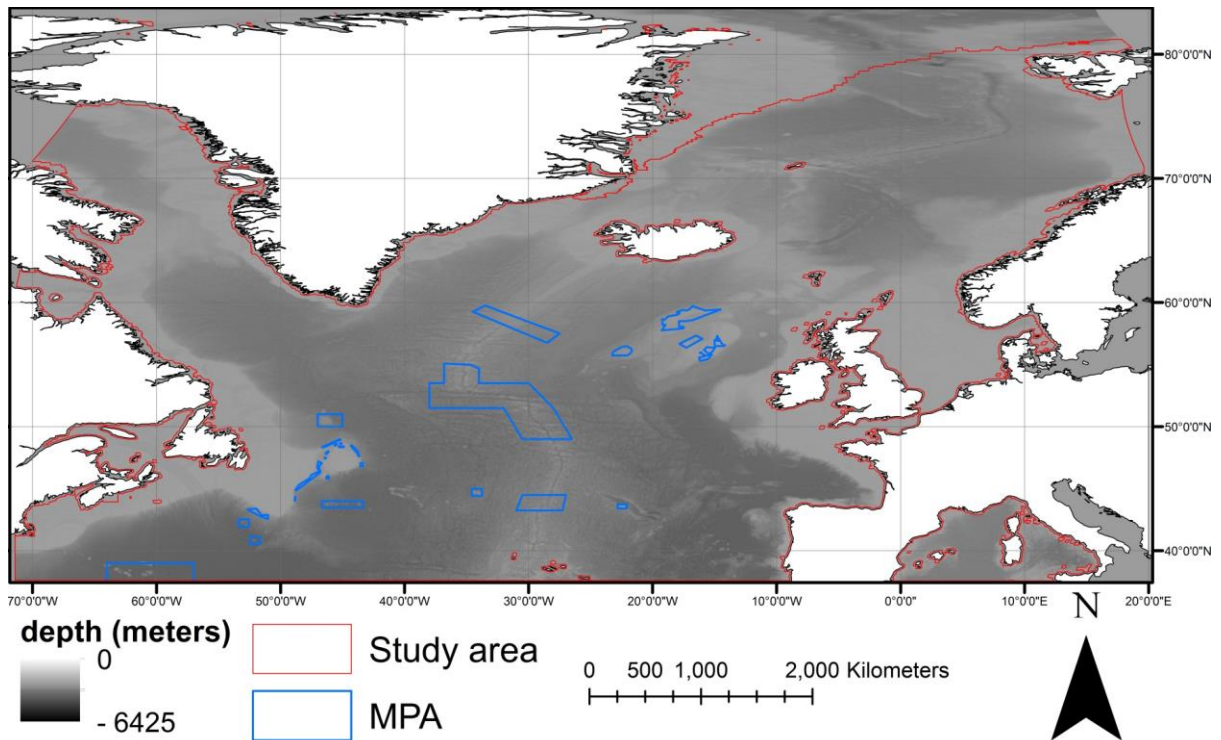
975

976 Table 5: Percentage of resource according to each model within the NAFO MPA
 977 network.

	% total area Geodia4+	% total area OstH	% total area OstEns	% total area <i>P.carpenteri</i>
percentage of High Seas resource within MPA	1.50%	19.44%	13.17%	13.49%
percentage of total resource within MPAs	0.06%	1.54%	0.07%	2.87%
percentage of MPAs total surface where the resource is present	0.22%	4.46%	0.08%	8.53%

978

979

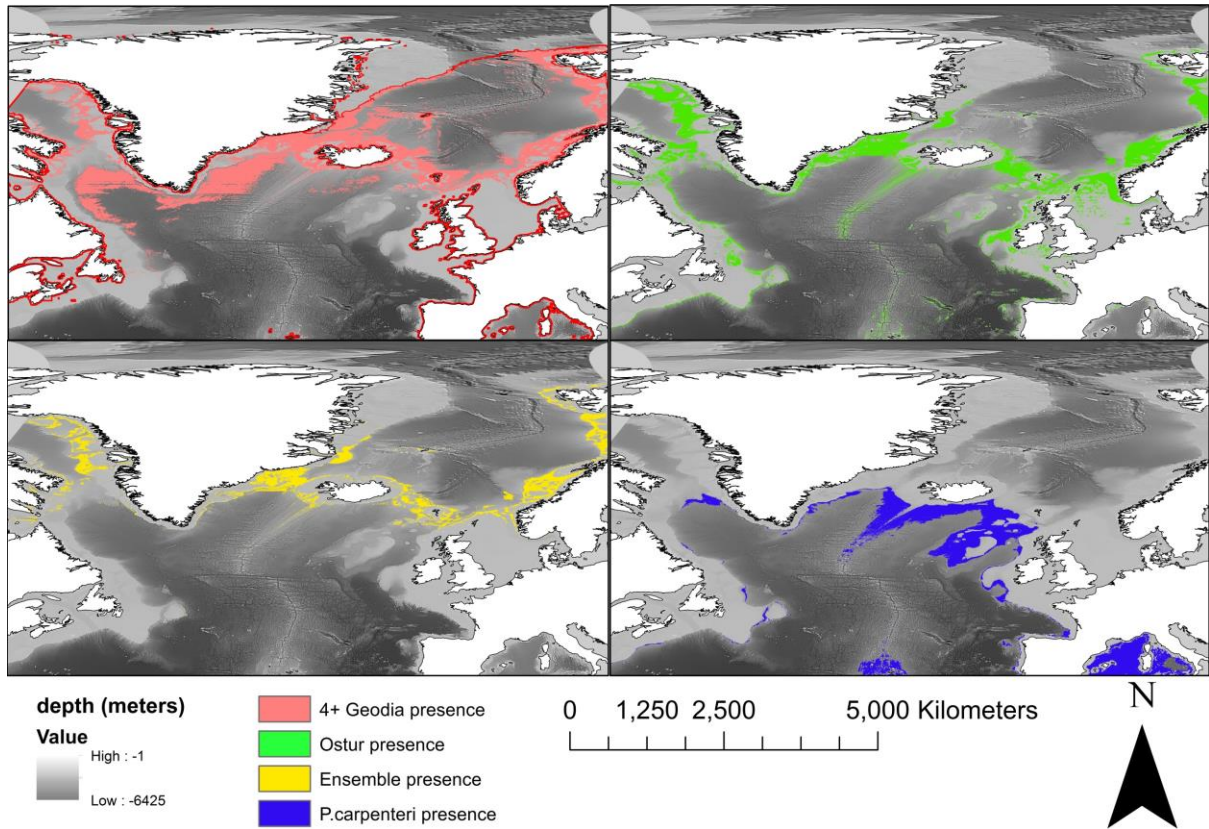


980

981 Figure 1: Full extent of the study area. The red line indicates the border of the modelled area.

982 Map projected in WGS 1984.

983



984

985 Figure 2: distribution maps of co-occurrence of: a) 4 or more Geodia species, b) presence of
 986 ostur habitat, c) presence of both 4 Geodia species and ostur habitat (ensemble model), and
 987 d) presence of *P. carpenteri* in the study area. Map projected in WGS 1984.